An Adaptive Generalized/eXtended FEM For Linear Elastic Fracture Mechanics

Murilo H. C. Bento[1], Sergio P. B. Proença[1], C. Armando Duarte[2]

[1]*Department of Structural Engineering, São Carlos School of Engineering, University of São Paulo*
Av. Trabalhador São-Carlense 400, 13566-590, São Carlos SP, Brazil
m.bento@usp.br, persival@sc.usp.br
[2]*Department of Civil and Environmental Engineering, University of Illinois Urbana-Champaign*
205 North Mathews Avenue, 61801, Urbana IL, USA
caduarte@illinois.edu

Abstract. The Generalized/eXtended Finite Element Method (G/XFEM) has been recognized as a method able to accurately and efficiently solve problems that face difficulties when treated by standard methodologies, such as those from three-dimensional (3-D) Linear Elastic Fracture Mechanics (LEFM). The main advantages of G/XFEM for this class of problems are the fact that the finite element mesh does not need to fit the crack surface and that optimal convergence rates in the energy norm are attained. This last advantage has been demonstrated for two-dimensional (2-D) problems even when uniform meshes are adopted. For 3-D, however, in addition to using enrichment functions, it has been shown that mesh refinement must be performed to obtain optimal convergence rates. In this case, since the level of refinement to be adopted is problem-dependent and difficult to be defined a priori, this work proposes an h-adaptive strategy, based on a posteriori error estimation, able to find optimal non-uniform meshes that recover optimal convergence rates for 3-D LEFM problems. This is shown herein for a LEFM problem that exhibits 3-D effects.

Keywords: G/XFEM, A posteriori error estimation, h-Adaptivity, 3-D LEFM

1 Introduction

The Generalized/eXtended Finite Element Method (G/XFEM), see Duarte et al. [1], Strouboulis et al. [2], and Belytschko and Black [3], has been recognized as a method able to accurately and efficiently solve problems that face difficulties when treated by standard methodologies. Three-dimensional (3-D) problems of Linear Elastic Fracture Mechanics (LEFM) are known to be challenging to the Finite Element Method (FEM) since (i) the mesh needs to fit the crack surface and (ii) special treatments, such as mesh refinement or special finite elements, need to be adopted close to the crack front in order to capture well the crack singularity. For this class of problems, the G/XFEM overcomes both these issues by inserting into the problem numerical approximation enrichment functions that accurately represent their discontinuous and singular behaviors.

For 3-D problems, however, Sanchez-Rivadeneira et al. [6] showed that in addition to using enrichment functions, mesh refinement is still needed close to crack fronts, especially when second- or higher-order G/XFEM formulations are adopted. This happens since the enrichment functions usually adopted within the G/XFEM are able to accurately represent the $\sqrt{r}$ singularity, but no higher-order singularities. While mesh refinement is much easier to be performed in G/XFEM than in FEM, the level of refinement for complex fracture problems is difficult to be set a priori. In this work, an a posteriori error estimator proposed in Bento et al. [11, 12] for 3-D LEFM problems is adopted and an h-adaptive algorithm able to recover optimal convergence rates through mesh refinement for these problems is initially proposed.

In what follows, Sections 2 and 3 briefly summarize the second-order pFEM-GFEM and the a posteriori ZZ-BD error estimator used in this work. Next, Section 4 presents the h-adaptive algorithm proposed in this work, which is essentially a specialization to LEFM problems of what is presented in Zienkiewicz and Zhu [8]. Then, Section 5 illustrates the use of this h-adaptive technique for a LEFM problem that exhibits 3-D effects, and, finally, Section 6 gives the main conclusions.

2 G/XFEM for 3-D Linear Elastic Fracture Mechanics

In this work, the h-adaptive algorithm is proposed to be used along with second-order G/XFEM formulations. It is noted that Sanchez-Rivadeneira and Duarte [4] showed that first-order G/XFEM is not competitive with second-order FEM that uses quarter-point elements. Due to this conclusion, recent works, such as the ones in Sanchez-Rivadeneira and Duarte [4] and Bento et al. [5], developed second-order G/XFEM formulations in which the convergence rate is optimal, i.e., $\mathcal{O}(h^2)$, with h a refinement parameter. In the present work, the formulation proposed in Sanchez-Rivadeneira and Duarte [4], referred to as pFEM-GFEM, is adopted, but other second- or higher-order formulations can be used as well.

This formulation [4] expands p-hierarchical FEM such that the pFEM-GFEM approximation space is given by

$$\mathcal{S}_{p\text{FEM-GFEM}} = \mathcal{S}_{p\text{FEM}} + \mathcal{S}_{\text{ENR}} = \mathcal{S}_{p\text{FEM}} + \left(\mathcal{S}^D_{\text{ENR}} + \mathcal{S}^S_{\text{ENR}}\right), \tag{1}$$

with $\mathcal{S}_{p\text{FEM}}$ a p-hierarchical space that approximates the polynomial part of the problem solution and $\mathcal{S}_{\text{ENR}}$ an enriched space, which can be decomposed as $\mathcal{S}_{\text{ENR}} = \mathcal{S}^D_{\text{ENR}} + \mathcal{S}^S_{\text{ENR}}$, for LEFM problems. In Eq. (1), $\mathcal{S}^D_{\text{ENR}}$ represents the discontinuous part of the displacement solution and $\mathcal{S}^S_{\text{ENR}}$ the singular and discontinuous part of the displacement solution of LEFM problems.

Since second-order discontinuous and singular basis functions are inserted into the numerical approximation, the pFEM-GFEM allows (i) the mesh to be generated independently of the crack surface and (ii) optimal convergence rates to be attained. Yet, well-conditioned stiffness matrices are obtained, as shown in Sanchez-Rivadeneira and Duarte [4]. For more details about pFEM-GFEM, the reader is reffered to Sanchez-Rivadeneira and Duarte [4], Sanchez-Rivadeneira et al. [6], and Mazurowski et al. [7].

3 A ZZ-BD Error Estimator for 3-D LEFM

Zienkiewicz and Zhu (ZZ) error estimators are recovery-based error estimators that compute approximations to the energy norm of the discretization error ϵ^* by substituting exact gradient fields by a recovered or improved gradient field. In the case of elasticity problems, this gradient field is usually taken as the stresses, and, once the recovered stresses are computed, the estimated error ϵ^* is given by

$$\epsilon^* = \sqrt{\int_\Omega \left(\mathcal{D}\left(\sigma^* - \hat{\sigma}\right)\right) \cdot \left(\sigma^* - \hat{\sigma}\right) \mathrm{d}V}, \tag{2}$$

with σ^* the recovered stress field and $\hat{\sigma}$ the approximated stress field.

Recently, based on the seminal work of Zienkiewicz and Zhu [8], Lins et al. [9] adapted this well-known ZZ estimator using a block-diagonal L^2 projection, proposed by Schweitzer [10], to compute the recovered stress field. The new error estimator proposed by Lins et al. [9], referred to as ZZ-BD (BD: block-diagonal), improves the error estimator computational performance, since the main matrix to be factorized is block-diagonal, while still returning good effectivity indexes. As follow-up works, Bento et al. [11] expanded the ideas to second-order FEM and G/XFEM and Bento et al. [12] developed error estimators for 3-D LEFM problems solved by the same second-order pFEM-GFEM as presented in Section 2.

In the present work, the ZZ-BD error estimator proposed in Bento et al. [12] to solve 3-D LEFM problems is used to guide h-adaptive simulations. In summary, as presented in Bento et al. [12], the recovered stress field for 3-D LEFM problems is given by

$$\sigma^*(\boldsymbol{x}) = \sigma^*_P(\boldsymbol{x}) + \sigma^*_D(\boldsymbol{x}) + \sigma^*_S(\boldsymbol{x}), \tag{3}$$

in which $\sigma^*_P(\boldsymbol{x})$ represents the polynomial part of the recovered stress field, generated by polynomial recovery enrichment functions, $\sigma^*_D(\boldsymbol{x})$ represents the discontinuous part of the recovered stress field, generated by high-order Heaviside recovery enrichment functions, and $\sigma^*_S(\boldsymbol{x})$ represents the singular part of the recovered stress field, generated by some terms of the gradients of Oden-Duarte (OD) enrichment functions, as proposed in Bento et al. [11].

For details, the reader is referred to Bento et al. [11, 12] to have a comprehensive explanation of the error estimator that is used next.

4 h-Adaptive Algorithm

The adaptive mesh refinement (AMR) framework proposed in Zienkiewicz and Zhu [8] and also presented in Oñate and Bugeda [13] is adopted in this work. This procedure consists of finding optimal finite element meshes in the sense that the discretization error becomes equally distributed over the finite elements. In summary, global and local adaptive criteria are defined and the associated global and local refinement parameters are computed, as presented in the following.

For the h-adaptive simulations performed in this work,

a) It is required the global discretization error ϵ to be smaller than or equal to a tolerance $\bar{\epsilon}$, i.e., $\epsilon \leq \bar{\epsilon}$. Based on this, a global discretization parameter ζ_G is defined as

$$\zeta_G = \frac{\epsilon}{\bar{\epsilon}}. \tag{4}$$

If $\zeta_G > 1$, all finite elements are uniformly refined.

b) It is also required the local discretization error ϵ_j, i.e., the discretization error in element j, with $j = 1, \ldots, N_{\text{el}}$, to be smaller than a required error ϵ_{r_j}. Since in this work, the h-adaptive algorithm seeks to equally distribute the discretization error over all finite elements, this required error is given by $\epsilon_{r_j} = \epsilon / \sqrt{N_{\text{el}}}$. Therefore, a local refinement parameter ζ_{L_j} is defined as

$$\zeta_{L_j} = \frac{\epsilon_j}{\epsilon}\sqrt{N_{\text{el}}}, \tag{5}$$

with N_{el} the number of elements.

For the definition of other local discretization parameters, the reader is referred to Oñate and Bugeda [13], for instance.

Based on these global and local refinement parameters, an element refinement parameter ζ_j can be computed as

$$\zeta_j = \zeta_G\,\zeta_{L_j} = \frac{\epsilon_j}{\bar{\epsilon}}\sqrt{N_{\text{el}}}. \tag{6}$$

Finally, for standard adaptive algorithms, the new finite element size h_j^{new} is obtained based on h_j^{old} as

$$h_j^{\text{new}} = \frac{h_j^{\text{old}}}{\beta_j}, \quad \beta_j = \left(\zeta_j\right)^{1/m}, \tag{7}$$

with $m = p$, and p the approximation polynomial order, except for finite elements that intersect singularities, in which $m = \lambda$, with λ the singularity strength.

4.1 h-Adaptivity for LEFM problems

In this work, an h-adaptive algorithm for LEFM problems is proposed based on what is presented in Section 4. One of the main assumptions is that the local refinement must be performed only close to the crack front, where the problem singularity lies. It is important to note that for 3-D LEFM problems, even when using enrichment functions as presented in Section 2, the singularity of order $\mathcal{O}(r^{3/2})$ still bounds the approximated second-order solutions. The h-adaptive procedure proposed herein is performed in two steps as summarized next:

1. The global refinement parameter ζ_G is computed using Eq. (4) and applied to refine all elements in the mesh; and, after that,

2. Local refinement parameters ζ_{L_j} are computed for the elements that touch or are intersected by the crack front and then an unique parameter β_{Γ_C} is obtained by

$$\beta_{\Gamma_C} = \max{}_{j \in S}\left(\beta_j\right), \tag{8}$$

with S a set containing all finite elements that touch or are intersected by the crack front and $\beta_j = \left(\zeta_G\,\zeta_{L_j}\right)^{1/m}$, computed as shown in Eqs. (6) and (5).

In Step 2, the parameter m is taken as $m = 3/2$ and β_{Γ_C} is the parameter used to compute h_j^{new} (cf. Eq. (7)) of all elements that touch or are intersected by the crack front.

5 Numerical Experiments

5.1 3-D Edge Crack Problem

The numerical example explored in this section consists of the following rectangular prism $\bar{\Omega} = [-0.5, 0.5] \times [-0.875, 0.875] \times [-0.75, 0.75] \subset \mathbb{R}^3$ containing a through-the-thickness edge crack

$$\bar{\Gamma}_C = \left\{ (x_1, x_2, x_3) \in \mathbb{R}^3 \,\middle|\, -0.5 \leq x_1 \leq 0, x_2 = 0, -0.75 \leq x_3 \leq 0.75 \right\},$$

as shown in Fig. 1. This is the same problem as the one analyzed in Sanchez-Rivadeneira et al. [6] and Bento et al. [12]. A linear elastic material, with Young's modulus $E = 1$ and Poisson's ratio $\nu = 0.3$, is adopted and uniform traction, with magnitude $\sigma_0 = 0.0025$, is applied normal to the boundaries in which $x_2 = -0.875$ and $x_2 = 0.875$. These boundary conditions are also depicted in Fig. 1. Dirichlet boundary conditions are applied to restrict rigid body motion only. It is noted that this is a pure Mode I problem.

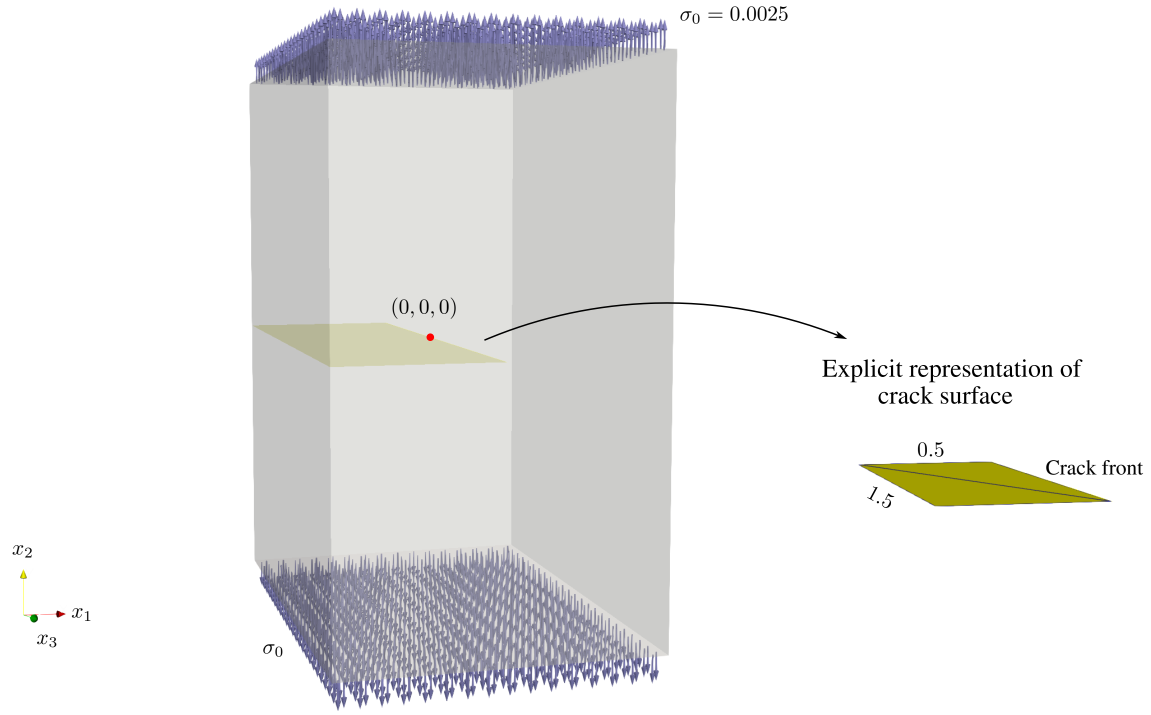

Figure 1. (a) Geometry and Neumann boundary conditions of the 3-D edge crack problem explored in this work, and (b) explicit representation of the crack surface. Figure extracted from Bento et al. [12]

In Bento et al. [12], the ZZ-BD error estimator presented in Section 3 is first presented for 3-D LEFM problems. As presented in Section 4, this error estimator is adopted in this work to guide h-adaptive simulations that seek to generate optimal meshes in the sense that optimal convergence rates of $\mathcal{O}({N_{\text{DoF}}}^{2/3})$ is obtained for 3-D LEFM problems too. As shown in Sanchez-Rivadeneira et al. [6], among others, in addition to adopting enrichment functions, mesh refinement around crack fronts is still required to attain optimal convergence rates for second- or higher-order G/XFEM formulations.

The numerical experiments shown in this section adopt $M^{(k)}$, with $k = 1, 2, 3$, as initial meshes to perform h-adaptive simulations and explore the procedure proposed in Section 4. Mesh $M^{(k)}$ is obtained by subdividing the edges parallel to x_1 by $8 \times k$, the edges parallel to x_2 by $14 \times k$, and the edges parallel to x_3 by $12 \times k$, and generating then uniform tetrahedral finite element meshes over the domain $\bar{\Omega}$. For all the meshes $M^{(k)}$, the corresponding finite element size is given by $h_k \equiv 1/(8k)$. The tetrahedral meshes $M^{(1)}$ and $M^{(2)}$ are depicted in Fig. 2.

The results presented in this section aim to initially test the h-adaptive algorithm proposed in Section 4 and check if it is able to recover optimal convergence rates for 3-D LEFM problems. Three h-adaptive simulations are

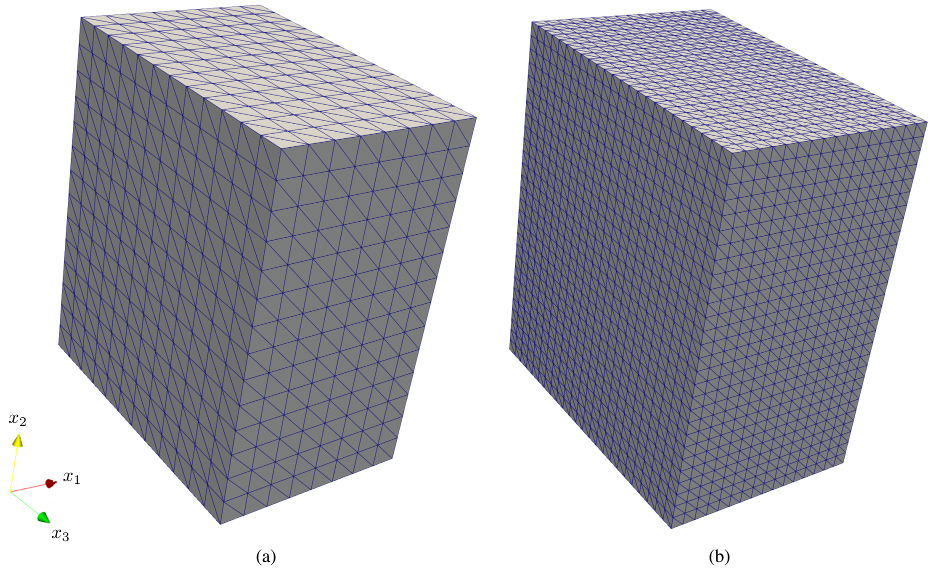

Figure 2. Uniform meshes (a) $M^{(1)}$ and (b) $M^{(2)}$ used as initial meshes for h-adaptive simulations. Mesh $M^{(3)}$, in which the edges parallel to x_1, x_2, and x_3 are divided by 24, 42, and 36, respectively, is also used as an initial mesh for h-adaptive simulation.

performed, each one starting with the uniform meshes $M^{(1)}$, $M^{(2)}$, and $M^{(3)}$. The tolerances $\bar{\epsilon}^{(k)}$ (see Section 4) are set so the h-adapted meshes are, after only global refinement, $M^{(2)}$, $M^{(3)}$, and $M^{(4)}$, respectively. These tolerances are computed, therefore, as

$$\bar{\epsilon}^{(k)} = \left(\frac{h^{(k+1)}}{h^{(k)}} \right)^2 \epsilon^{(k)}.$$

The values of $\bar{\epsilon}^{(k)}$ and the associated global refinement parameter $\zeta_G^{(k)} = \left(\frac{h^{(k+1)}}{h^{(k)}} \right)^{-2}$ (cf. Eq. (4)) are presented in Table 1.

It is importante to note here that usually $\bar{\epsilon}$ is an user pre-specified tolerance value. However, since the numerical experiments presented in this section aim to initially test the h-adaptive procedure proposed herein, the value $\bar{\epsilon}$ is computed so the h-adapted mesh related to $M^{(k)}$ is given by $M^{(k+1)}$.

Table 1. Summary of h-adaptive simulations performed in this work. Initial mesh and finite element size, and tolerances $\bar{\epsilon}^{(k)}$ are presented, as well as the global refinement parameter $\zeta_G^{(k)} = \epsilon^{(k)}/\bar{\epsilon}^{(k)}$.

Simulation (k)	**Initial Mesh**	$h^{(k)}$	Tolerance $\bar{\epsilon}^{(k)}$	$\zeta_G^{(k)}$
1	$M^{(1)}$	0.12500	8.10×10^{-5}	4.000
2	$M^{(2)}$	0.06250	6.97×10^{-5}	2.250
3	$M^{(3)}$	0.04167	4.81×10^{-5}	1.778

In summary, following what is presented in Section 4.1, the h-adaptive analysis (k) starts with uniform mesh $M^{(k)}$ and, after global refinement based on the global refinement parameter $\zeta_G^{(k)}$, the uniform mesh $M^{(k+1)}$ is obtained. After that, as presented in Section 4.1, local refinement is performed close to the crack front based on $\beta_{\Gamma_C}^{(k)}$. The values of $\beta_{\Gamma_C}^{(k)}$ is presented in Table 2.

Finally, Fig. 3 illustrates plots of $\epsilon \times N_{\text{DoF}}$ related to the performed h-adaptive simulations. The blue curve shows the convergence curve when only uniform meshes are adopted. It is observed that the h-adaptive simulations are able to recover optimal convergence rates, which is $\mathcal{O}({N_{\text{DoF}}}^{2/3})$. All simulations performed herein use estimated errors, but the dashed curves in Fig. 3 show also the associated reference errors. These reference

Table 2. Parameters adopted to refine the mesh close to the crack front.

Simulation (k)	**Initial Mesh**	$\beta_{\Gamma_C}^{(k)}$	New mesh size close to the crack front $h^{\text{new},(k)} = h^{\text{old},(k)}/\beta_{\Gamma_C}^{(k)}$
1	$M^{(1)}$	1.241×10^1	1.01×10^{-2}
2	$M^{(2)}$	1.690×10^1	3.70×10^{-3}
3	$M^{(3)}$	2.389×10^1	1.74×10^{-3}

errors are obtained by Eq. (2), substituting the recovered field σ^* by the exact one σ. The closeness between the corresponding curves shows the good effectivity of the ZZ-BD error estimator to estimate discretization errors, as shown in Bento et al. [12].

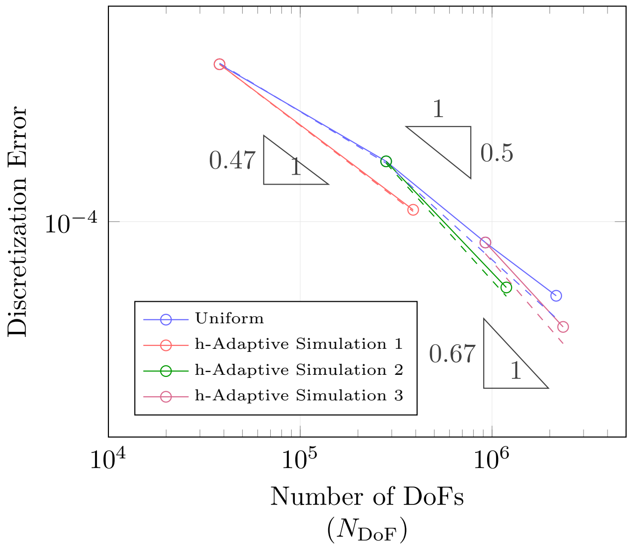

Figure 3. h-Adaptive simulations (red, green, and purple curves) performed aiming to recover optimal convergence rates for the 3-D edge crack problem, which is $\mathcal{O}({N_{\text{DoF}}}^{2/3})$. The results shown as a blue curve use only uniform meshes and sub-optimal convergence rates are obtained in this case.

6 Conclusions

In this work, an h-adaptive procedure that explores the ZZ-BD error estimator is presented. The procedure essentially uses estimated discretization errors and an adaptive mesh refinement criteria to find optimal non-uniform meshes that recover optimal convergence for 3-D LEFM problems. The results shown herein are a first indication that optimal convergence of second-order G/XFEM approximations can be achieved for LEFM problems that exhibits 3-D effects through the use of adaptive algorithms. As follow-up works, more complex LEFM problems with non-trivial crack surfaces will be investigated.

Acknowledgements. Murilo H. C. Bento and Sergio P. B. Proença gratefully acknowledge the support provided by the University of São Paulo and the financial support provided by the São Paulo Research Foundation (FAPESP), grant 2019/00435-3.

Authorship statement. The authors hereby confirm that they are the sole liable persons responsible for the authorship of this work, and that all material that has been herein included as part of the present paper is either the property (and authorship) of the authors, or has the permission of the owners to be included here.

References

[1] C. A. Duarte, I. Babuška, and J. T. Oden. Generalized finite element methods for three-dimensional structural mechanics problems. *Computers and Structures*, vol. 77, pp. 215–232, 2000.

[2] T. Strouboulis, I. Babuška, and K. Copps. The design and analysis of the Generalized Finite Element Method. *Computer Methods in Applied Mechanics and Engineering*, vol. 181, n. 1–3, pp. 43–69, 2000.

[3] T. Belytschko and T. Black. Elastic crack growth in finite elements with minimal remeshing. *International Journal for Numerical Methods in Engineering*, vol. 45, pp. 601–620, 1999.

[4] A. G. Sanchez-Rivadeneira and C. A. Duarte. A stable generalized/extended FEM with discontinuous interpolants for fracture mechanics. *Computer Methods in Applied Mechanics and Engineering*, vol. 345, pp. 876–918, 2019.

[5] M. H. C. Bento, S. P. B. Proença, and C. A. Duarte. Well-conditioned and optimally convergent second-order Generalized/eXtended FEM formulations for linear elastic fracture mechanics. *Computer Methods in Applied Mechanics and Engineering*, vol. 394, pp. 114917, 2022.

[6] A. G. Sanchez-Rivadeneira, N. Shauer, B. Mazurowski, and C. A. Duarte. A Stable Generalized/eXtended p-hierarchical FEM for three-dimensional linear elastic fracture mechanics. *Computer Methods in Applied Mechanics and Engineering*, vol. 364, pp. 112970, 2020.

[7] B. Mazurowski, A. G. Sanchez-Rivadeneira, N. Shauer, and C. A. Duarte. High-order stable generalized/extended finite element approximations for accurate stress intensity factors. *Engineering Fracture Mechanics*, vol. 241, pp. 107308, 2021.

[8] O. C. Zienkiewicz and J. Z. Zhu. A simple error estimator and adaptive procedure for practical engineering analysis. *International Journal for Numerical Methods in Engineering*, vol. 24, pp. 337–357, 1987.

[9] R. M. Lins, S. P. B. Proença, and C. A. Duarte. Efficient and accurate stress recovery procedure and a posteriori error estimator for the stable generalized/extended finite element method. *International Journal for Numerical Methods in Engineering*, vol. 119, n. 12, pp. 1279–1306, 2019.

[10] M. Schweitzer. Variational mass lumping in the Partition of Unity Method. *SIAM Journal of Scientific Computing*, vol. 35, pp. A1073–A1097, 2013.

[11] M. H. C. Bento, S. P. B. Proença, and C. A. Duarte. Recovery strategies, a posteriori error estimation, and local error indication for second-order G/XFEM and FEM. *International Journal for Numerical Methods in Engineering*, vol. 124, n. 13, pp. 3025–3062, 2023a.

[12] M. H. C. Bento, S. P. B. Proença, and C. A. Duarte. A posteriori error estimation for second-order optimally convergent G/XFEM. In F. Larsson and P. Díez, eds, *Proceedings of the XI International Conference on Adaptive Modeling and Simulation*, pp. 1–8. CIMNE, 2023b.

[13] E. Oñate and G. Bugeda. A study of mesh optimality criteria in adaptive finite element analysis. *Engineering Computations*, vol. 10, pp. 307–321, 1993.